the plant journal

SEB SOCIETY FOR EXPERIMENTAL BIOLOGY

The Plant Journal (2023) doi: 10.1111/tpj.16232

A *Phytophthora infestans* RXLR effector AVR8 suppresses plant immunity by targeting a desumoylating isopeptidase DeSI2

Rui Jiang[1,2,†], Qin He[1,†], Jingyi Song[1,†], Zeng Liu[1], Jian Yu[1], Kefan Hu[1,3], Huiming Liu[1], Yang Mu[1], Jiahui Wu[1], Zhendong Tian[1], Botao Song[1], Vivianne G. A. A. Vleeshouwers[4], Conghua Xie[1] and Juan Du[1,*]

[1]*National Key Laboratory for Germplasm Innovation & Utilization of Horticultural Crops, Key Laboratory of Potato Biology and Biotechnology, Ministry of Agriculture and Rural Affairs, Huazhong Agricultural University, Wuhan 430070, China,*

[2]*Chongqing Key Laboratory of Biology and Genetic Breeding for Tuber and Root Crops, Engineering Research Center of South Upland Agriculture, Ministry of Education, Southwest University, Chongqing 400715, China,*

[3]*Department of Biology, Hong Kong Baptist University, Hong Kong, Hong Kong Special Administrative Region (HKSAR), China, and*

[4]*Plant Breeding, Wageningen University and Research, Droevendaalsesteeg 1, Wageningen 6708 PB, The Netherlands*

Received 7 July 2022; revised 27 February 2023; accepted 28 March 2023.
*For correspondence (e-mail juandu@mail.hzau.edu.cn).
†These authors contributed equally to this work.

SUMMARY

The potato's most devastating disease is late blight, which is caused by *Phytophthora infestans*. Whereas various resistance (*R*) genes are known, most are typically defeated by this fast-evolving oomycete pathogen. However, the broad-spectrum and durable *R8* is a vital gene resource for potato resistance breeding. To support an educated deployment of *R8*, we embarked on a study on the corresponding avirulence gene *Avr8*. We overexpressed *Avr8* by transient and stable transformation, and found that *Avr8* promotes colonization of *P. infestans* in *Nicotiana benthamiana* and potato, respectively. A yeast-two-hybrid (Y2H) screen showed that AVR8 interacts with a desumoylating isopeptidase (StDeSI2) of potato. We overexpressed *DeSI2* and found that *DeSI2* positively regulates resistance to *P. infestans*, while silencing *StDeSI2* downregulated the expression of a set of defense-related genes. By using a specific proteasome inhibitor, we found that AVR8 destabilized StDeSI2 through the 26S proteasome and attenuated early PTI responses. Altogether, these results indicate that AVR8 manipulates desumoylation, which is a new strategy that adds to the plethora of mechanisms that *Phytophthora* exploits to modulate host immunity, and StDeSI2 provides a new target for durable resistance breeding against *P. infestans* in potato.

Keywords: potato, *Phytophthora infestans*, plant immunity, effector, AVR8, desumoylating isopeptidase, StDeSI2.

INTRODUCTION

Worldwide, late blight caused by *Phytophthora infestans* is the most devastating disease for potato, and seriously affects yield and quality. Breeding resistant varieties is the most economical and effective method in potato production. Till now, nucleotide-binding leucine-rich repeat (*NLR*) genes have been widely used for potato late blight resistance breeding, and more than 20 *NLR* genes have been cloned in potatoes in recent 20 years (Du & Vleeshouwers, 2017; Witek et al., 2021). The resistance conferred by most *NLR* genes against late blight is typically short lived (Vleeshouwers et al., 2011), but *R8* has been proven to be one of the few genes with broad-spectrum and more durable resistance (Jiang et al., 2018; Rietman et al., 2012; Vossen et al., 2016).

The 240-MB genome of *P. infestans* contains about 560 RXLR effector genes with high plasticity and rapid evolution, resulting in evolving new isolates to overcome the deployed *NLR* genes (Dong et al., 2014; Fry, 2008; Haas et al., 2009; McDonald & Linde, 2002; Raffaele et al., 2010; Vleeshouwers et al., 2011). Understanding how pathogens manipulate hosts by the action of RXLR effectors enhances our knowledge of the infection process and can help us develop disease-resistance crops (Gawehns et al., 2013; van Schie & Takken, 2014). RXLR effectors have N-terminal signal peptides and RXLR regions that mediate secretion

and translocation into host cells (He, Ye, et al., 2019; Whisson et al., 2007; Win et al., 2012). The virulence activities of over a dozen *P. infestans* RXLR effectors have been functionally characterized (He et al., 2020; Petre et al., 2021). For example, AVR1 and AVRblb2 prevent the secretion of host proteins (Bozkurt et al., 2011; Du et al., 2015). AVR2 targets BRASSINOSTEROID INSENSITIVE 1 (BRI1)-SUPPRESSOR1-like (BSL) family members in potato, which are phosphatases that regulate brassinosteroid signaling to suppress host immunity (Turnbull et al., 2017; Turnbull et al., 2019). Pi04314 targets plant phosphatases to suppress transcriptional responses regulated by the hormones JA and SA (Boevink et al., 2016). PexRD54/Pi09316 stimulates the formation of autophagosomes at the pathogen interface (Dagdas et al., 2016; Dagdas et al., 2018; Pandey et al., 2021). AVR3a and SFI5 require association with an E3 ligase and calmodulin, respectively, to suppress pathogen-associated molecular pattern (PAMP)-triggered immunity (PTI; Bos et al., 2006, 2010; Gilroy et al., 2011; Zheng et al., 2018). PiSFI3/Pi06087/PexRD16 targets a plant U-Box-kinase protein (StUBK) to suppress immunity (He, McLellan, et al., 2019). PexRD2/Pi11383 and Pi22926 inhibit the kinase activity (King et al., 2014; Ren et al., 2019). Pi02860, Pi04089, Pi17316, AVRblb2 (Pi20300) and its virulent variant Pi20303 target host susceptibility factors to promote late blight disease (Du et al., 2020; He et al., 2018; Murphy et al., 2018; Wang et al., 2015). However, according to our knowledge, the virulence function of AVR8 has not been reported so far.

Sumoylation is a post-translational modification of proteins that is essential for the normal function of eukaryotes. In plants, sumoylation modification is basically involved in all physiological processes, including abiotic stress, abscisic acid signaling, development, flowering time control, and immune regulation (Park et al., 2011). The covalent modification of proteins by SUMO is reversible. By hydrolyzing the isopeptide bond between SUMO and substrate, SUMO can be removed from its target protein, which is called desumo. *Arabidopsis* SUMO proteases are classified into two distinct groups of cysteine proteases, namely ubiquitin-like protease (Ulp) and deSUMOylating isopeptidase (DeSI) families (Nayak & Muller, 2014). Ulps belong to the C48 subgroup of the CE superfamily characterized by a catalytic triad His-Asp-Cys, whereas DeSIs belong to the C97 subgroup and possess the catalytic dyad His-Cys (Hickey et al., 2012). They are responsible for the activation of pre-SUMO into mature SUMO and SUMO deconjugation, respectively (Yates et al., 2016). Desumoylated isopeptidases in mice mainly contain DeSI-1 and DeSI-2, which share 23% homology at the amino acid level (Shin et al., 2012). In *Arabidopsis*, the DeSI family has further evolved and can be divided into four categories (Orosa et al., 2018). At present, the only report of DeSI in plant immunity is that DeSI3a located on the cell membrane can desumo FLAGELLIN-SENSITIVE 2 (FLS2) in *Arabidopsis*, inhibiting the dissociation of BIK1 from the pattern recognition receptor complex, which inhibits the transcriptional response downstream of FLS2 (Orosa et al., 2018).

This study focuses on the virulence function of the RXLR effector AVR8. We found that *Avr8* promotes the disease development of *P. infestans*. Through yeast-two-hybrid (Y2H), co-immunoprecipitation (Co-IP) and split luciferase assays, we identified an AVR8 key target protein StDeSI2 that plays a positive regulatory role in the resistance of potato late blight. AVR8 can degrade StDeSI2 through the 26S proteasome and then attenuate early PTI responses. These findings point to a new strategy by which oomycete pathogens regulate host defense and manipulate sumoylation-related proteins.

RESULTS

Avr8 promotes the colonization of *Phytophthora infestans*

To test whether *Avr8* can promote the colonization of *P. infestans*, N-terminal GFP-tagged *Avr8* was transiently expressed in the leaves of *Nicotiana benthamiana* via agroinfiltration. Then leaves were detached and spot-inoculated with a zoospore suspension of *P. infestans* isolate 88069, and lesions were measured at 7 days post-inoculation (dpi). The results showed that lesion areas were significantly larger on *Avr8*-treated leaves compared with the GFP control (Figure 1a–c).

To further confirm the influence of *Avr8* on its host, *Myc-Avr8* was transformed ectopically in the potato cultivar Désirée (Figure 1d). *Phytophthora infestans* isolate 88069 was used for the infection assay on detached leaves. Two Désirée-*Myc-Avr8* transformants displayed significantly enhanced lesion areas compared with the Désirée control (Figure 1e). In line with the findings with other *Avr* genes from *P. infestans*, these results further confirmed that ectopically expressed *Avr8* promotes *P. infestans* colonization (Wang et al., 2019).

AVR8 interacts with a putative desumoylating isopeptidase DeSI2

To identify the host target of AVR8, AVR8 without signal peptide was used as bait to screen a Y2H cDNA library that was previously established by the leaves of the potato cultivar Désirée infected with *P. infestans* (McLellan et al., 2013). However, no yeast colonies were recovered from the selection plates. Then we used the effector domain (ED)$^{58–243\ aa}$ of AVR8 as bait to screen the same Y2H cDNA library three times. In total, five independent positive clones were obtained. The resulting sequences suggest that every single clone encodes the same gene, a putative *desumoylating isopeptidase* (*DeSI*), of which the nucleotide sequences are the same.

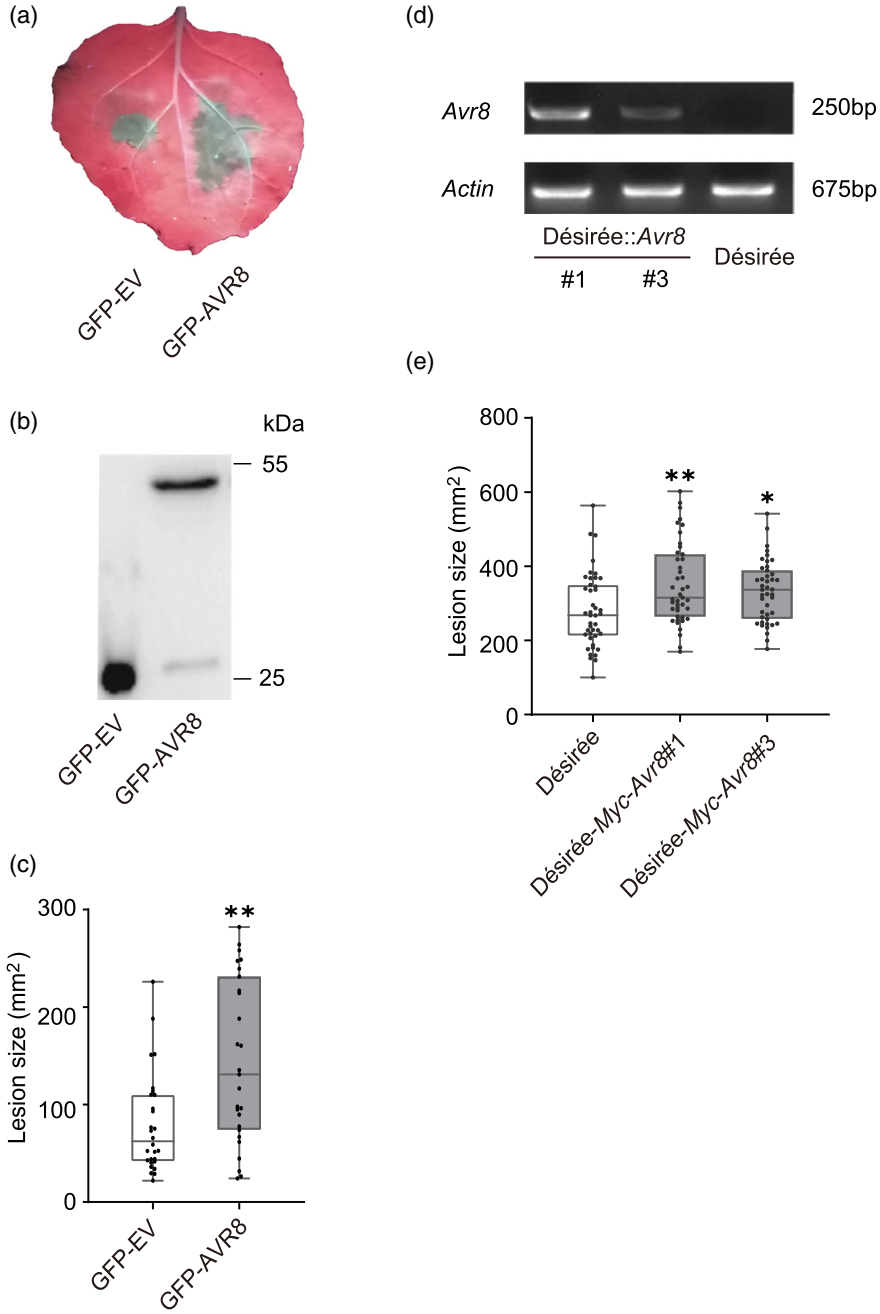

Figure 1. *Avr8* promotes the colonization of *Phytophthora infestans* in both *Nicotiana benthamiana* and potato.
(a) Representative photographs of *N. benthamiana* leaves infected with a *P. infestans* isolate 88069 following agroinfiltration of *GFP* empty vector (*GFP*-EV) on the left side and *GFP-Avr8* constructs on the right side of the midvein. Photographs were taken at 7 days post-infection (dpi).
(b) Immunoblot analysis shows that recombinant GFP-AVR8 protein is intact *in planta*. The protein size is indicated on the right panel in kDa.
(c) The mean lesion size is significantly larger with the agroinfiltration of *GFP-Avr8* than that of *GFP-EV* in *N. benthamiana* leaves. The lesion size data are shown as means with SD ($n \geq 27$).
(d) The expression level of *Avr8* in transgenic potato cv Désirée. Reverse transcriptase-polymerase chain reaction (RT-PCR) analysis shows that *Avr8* is specifically expressed in Désirée-*Avr8* transformants #1 and #3. *Actin* expression level quantified cDNA abundance in the lower panel.
(e) The mean lesion size is significantly larger in leaves of Désirée-*Avr8* transformants #1 and #3 than that in the Désirée control leaves infected with 88069 at 5 dpi. The lesion size data are shown as means with SD ($n = 43$). Independent experiments have been conducted at least three times with similar results. Student's *t*-test was used for the statistical analysis, $*P < 0.05$, $**P < 0.01$.

The unique Peptidase_C97 (PF05903) domains of DeSI family members comprise 151 amino acids, and in total nine proteins were identified in potato based on HMMER searches (E-value $< 1 \times 10^{-5}$). To clarify which *DeSI* was identified, we constructed a phylogenetic tree of all *DeSI* family members from human, *Arabidopsis*, potato and *N.*

benthamiana. We designated the identified *DeSI* from potato as *StDeSI2*, which is close to *AtDeSI2* (Figure S1).

Then, we endeavored to verify the Y2H interaction of AVR8 and StDeSI2. The full length of *StDeSI2*, encoding a protein of 234 amino acids (aa), was cloned into the prey construct, while the full length and the ED of *Avr8* were cloned into the cognate bait construct. AVR2 was used as a negative control. As shown in Figure 2a, ED strongly interacts with StDeSI2, while the interaction is much weaker for AVR8 and StDeSI2. This could be the reason why StDeSI2 was not caught by AVR8 through the Y2H assay.

To further confirm the interaction between AVR8 and StDeSI2, a Co-IP was performed using N-terminal GFP-tagged AVR8, co-expressing with N-terminal HA-tagged StDeSI2 *in planta*. HA-StDeSI2 was detected by the HA antibody when co-immunoprecipitated with GFP-AVR8, while not with the GFP empty vector (Figure 2b). To verify the interaction between AVR8 and StDeSI2, a split luciferase assay was performed using SA receptors NPR3-nluc and cluc-NPR4 combination as a positive control (Liu et al., 2016). The signal of luciferase catalytic activity restored by AVR8 and StDeSI2 was even stronger than the positive control, while no signals were detected for the AVR2 and StDeSI2 combination and negative control (Figure 2c,d). Taken together, we show that AVR8 physically interacts with StDeSI2 both *in vivo* and *in vitro*.

We further investigated the subcellular localization of AVR8 and StDeSI2. *Agrobacterium* transformed with *GFP-Avr8* and *RFP-StDeSI2* constructs were infiltrated in *N. benthamiana* leaves, separately or together. Confocal microscopy scans show that both GFP-AVR8 and GFP-StDeSI2 localize in the cytoplasm, and co-expressing GFP-AVR8 and RFP-StDeSI2 does not change their localization

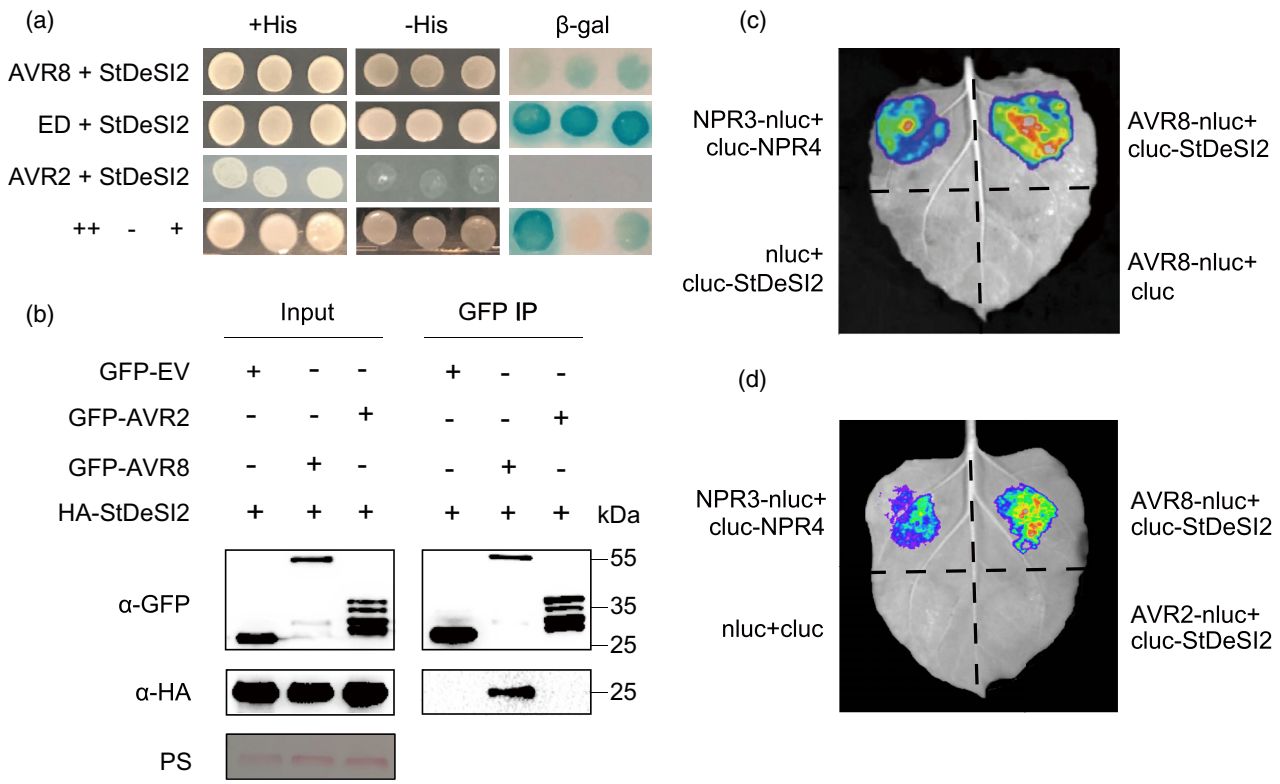

Figure 2. AVR8 interacts with a putative desumoylating isopeptidase (StDeSI2).
(a) Both AVR8 and its effector domain (ED) interact with StDeSI2 in yeast. The bait vector pDEST32 carrying each of *Avr8*, *ED* and *Avr2* was co-transformed with the prey vector carrying *StDeSI2* into the yeast strain Mav203 competent cells, respectively. Transformants carrying both prey and bait vectors were grown on selective medium SD/-Trp/Leu and SD/-Trp/-Leu/-His. SD, yeast synthetic dropout medium. AVR2 construct was used as a negative control. Yeast controls in the ProQuest™ Two-Hybrid System are indicated as ++, +, and –, which stand for strong interaction, weak interaction, and no interaction, respectively.
(b) AVR8 interacts with StDeSI2 *in vivo*. N-terminal *GFP*-tagged *Avr8* and N-terminal *HA*-tagged *StDeSI2* were co-infiltrated in *Nicotiana benthamiana*. GFP-AVR2 or GFP-EV with HA-StDeSI2 constructs were used as negative controls. Samples were collected 48 h post-infiltration. Crude proteins were used as input, and proteins immunoprecipitated with GFP-Trap were used as output. Western blot was performed using anti-GFP and anti-HA antibodies, and protein markers were shown on the right panel in kDa.
(c, d) AVR8 interacts with StDeSI2 *in planta*. Split luciferase construct pairs NPR3-nluc/cluc-NPR4, AVR8-nluc/cluc-StDeSI2, nluc/cluc-StDeSI2, AVR8-nluc/cluc, AVR2-nluc/cluc-StDeSI2 and nluc/cluc were co-expressed in *N. benthamiana*. Luciferin was applied on the *N. benthamiana* leaves at 48 h post-infiltration. Luminescence photos were captured using a CCD imaging apparatus 10 min later. AVR8-nluc/cluc-StDeSI2 shows a stronger signal than the positive control NPR3-nlu/cluc-NPR4 on the upper side of the leaf, while all the negative controls do not show any signals.

(Figure 3a,b). Western blot results showed that the fusion protein of GFP-AVR8 and RFP-StDeSI2 was intact in *N. benthamiana* (Figure 3c).

Silencing of *DeSI2* does not affect R8/AVR8 cell death response

To detect whether DeSI2 plays a role in R8/AVR8 cell death response, we performed virus-induced gene silencing (VIGS) to silence *DeSI2* in *N. benthamiana*. This plant contains two DeSI2 homologs, NbDeSI2A and NbDeSI2B, which share similarities of 90.1% and 90.5% to the StDeSI2 protein, respectively (Figure S1; Table S2). A conserved fragment of 304 bp was designed to silence both *NbDeSI2A* and *NbDeSI2B* (Figure S2a). Leaves of 2-week-old plants were treated with TRV-*NbDeSI2* and the control TRV-*GFP*, respectively. TRV-*PDS*-treated plants were used as environmental control. After 3 weeks, there were no obvious changes in the phenotype of TRV-*NbDeSI2*-treated plants compared with the control TRV-*GFP*-treated plants (Figure S2b). The silencing efficiency of *NbDeSI2* was

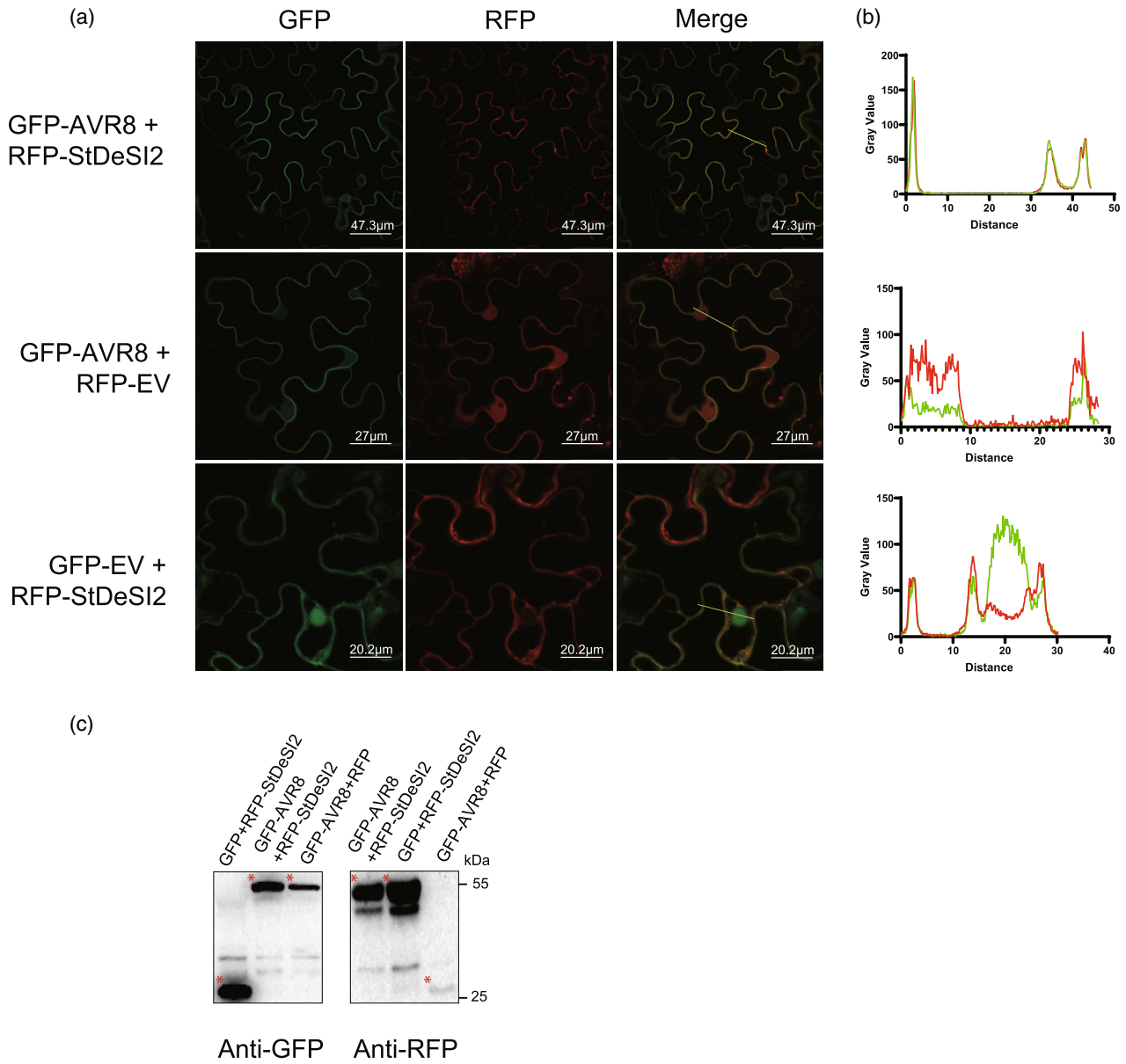

Figure 3. AVR8 and StDeSI2 co-localize in the cytoplasm.
(a) Fluorescence images show that AVR8 and StDeSI2 co-localize in the cytoplasm of *Nicotiana benthamiana* at 48 h post-infiltration. AVR8 or StDeSI2 alone also localize in the cytoplasm. Scale bars are presented in the bottom right.
(b) The fluorescence intensity plot verifies the co-localization of AVR8 (green) and StDeSI2 (red). *x*-axis, distance; *y*-axis, fluorescence intensity.
(c) Immunoblot shows the expression of the proteins expressed in panel (a).

tested by quantitative reverse transcriptase-polymerase chain reaction (qRT-PCR), and the result shows that its transcript level was reduced to 15–30% (Figure S2c).

The TRV-treated leaves were infiltrated with a mixture of the *Agrobacterium* strain GV3101 containing pB7WGF2-R8/pB7WGF2-AVR8 (Jiang et al., 2018), pB7WGF2-Cf-4/pB7WGF2-Avr4 (Joosten et al., 1994), pGR106-INF1, and empty vectors pGR106-EV and pB7WGF2-EV (negative control), as well as *P. infestans* culture filtrate (CF; Figure S3a). As a result, R8/AVR8, Cf-4/Avr4, INF1 and CF triggered cell death responses on TRV-*NbDeSI2*-treated *N. benthamiana* leaves (Figure S3b) as well as on TRV-*GFP* control plants (Figure S3c), while their empty vectors pGR106-EV and pB7WGF2-EV that were used as negative controls did not trigger any obvious symptoms. These results indicate that DeSI2 may not be involved in the *R8*-mediated signaling pathway.

Silencing of *DeSI2* promotes *P. infestans* colonization in *Nicotiana benthamiana* and potato

Then we tested if DeSI2 plays a role in the resistance against *P. infestans*. VIGS was performed again to silence *NbDeSI2*, and then the TRV-treated leaves were detached and spot-inoculated with a zoospore suspension of the compatible *P. infestans* isolate 88069. At 7 dpi, the mean lesion size of TRV-*NbDeSI2*-treated plants was significantly larger than that of the control TRV-*GFP*-treated plants in at least three independent experiments (Figure 4a–c). These results demonstrate that silencing *NbDeSI2* promotes *P. infestans* colonization in *N. benthamiana*.

To further examine the potential role of DeSI2 in the natural host of *P. infestans*, we generated an RNA interference construct of *StDeSI2* and transformed it into a susceptible potato cultivar Désirée. In total, eight Désirée-*StDeSI2* RNAi transformants were obtained, which did not show obvious changes in the phenotype compared with the control Désirée after growing 7 weeks in the pots (Figure S4a). Among them, the transcript level of *StDeSI2* in six transformants reduced below 25% compared with that in control Désirée plants, while that was about 50% in the other two transformants (Figure S4d).

To test whether the transformants display altered late blight disease susceptibility, we spot-inoculated zoospore suspensions of the compatible *P. infestans* isolates 88069 and EC-1 on detached mature leaves. At 5 dpi, the mean lesion size of Désirée-*StDeSI2* RNAi transformants was significantly larger than that of the control Désirée plants for both isolates in at least three independent experiments (Figures 4d,e and S4b,c). In line with this, the biomass of *P. infestans* was significantly increased in Désirée-*StDeSI2* RNAi transformants compared with the control Désirée at 5 dpi (Figure 4f). The *StDeSI2* expression level in the Désirée-*StDeSI2* RNAi transformants remained unchanged inoculated with *P. infestans* (Figure S4e). Altogether, these results demonstrate that silencing *StDeSI2* promotes *P. infestans* colonization in potato.

Overexpression of *StDeSI2* attenuates *Phytophthora infestans* colonization in *Nicotiana benthamiana* and potato

We also investigated the overexpression effect of *StDeSI2* against *P. infestans*. pH7LIC9.0-*Myc-StDeSI2* was agroinfiltrated in *N. benthamiana* leaves as well as pH7LIC9.0-*Myc-GUS*, which was used as a negative control. At 2 dpi, the StDeSI2 and GUS proteins were properly expressed (Figure 5c). Then, the agroinfiltrated leaves were detached and spot-inoculated with the *P. infestans* isolate 88069. At 7 dpi, the mean lesion size of *Myc-StDeSI2*-treated leaves was significantly smaller than that of the control *Myc-GUS*-treated leaves (Figure 5a,b). These results demonstrate that transient overexpression of *StDeSI2* reduces infection levels of *P. infestans* in *N. benthamiana*.

Then, we further generated stable transformants of *StDeSI2* of Désirée. In total, four Désirée-*StDeSI2* transformants were obtained, which did not show obvious changes in the phenotype compared with the control Désirée after growing 7 weeks in the pots (Figure S5a). Among them, the transcript level of *StDeSI2* in three transformants increased about six–eight times compared with that in the control Désirée plants, while that was doubled in Désirée-*StDeSI2* transformant#5 (Figure S5d). A zoospore suspension of each of two *P. infestans* isolates 88069 and EC-1 was used to spot-inoculate the detached mature leaves. At 5 dpi, the mean lesion size of Désirée-*StDeSI2* transformants was significantly smaller compared with control Désirée plants for both isolates in at least three independent experiments (Figures 5d,e and S5b,c). In line with this, the biomass of *P. infestans* was also significantly decreased in Désirée-*StDeSI2* overexpression transformants compared with the control Désirée at 5 dpi (Figure 5f). These results demonstrate that in line with the transient expression studies, overexpression of *StDeSI2* in stable potato transformants attenuates colonization of *P. infestans*.

AVR8 destabilizes StDeSI2 protein *in vivo*

To investigate the impact of AVR8 on StDeSI2, we co-infiltrated GFP-Avr8 and Myc-StDeSI2 into *N. benthamiana* leaves and examined the protein abundance of StDeSI2 using Western blot. Our results indicate that co-expression with AVR8 led to a significant reduction in StDeSI2 levels compared with co-expression with GFP (Figure 6a,b), suggesting that AVR8 may destabilize StDeSI2.

To test whether StDeSI2 is degraded via the 26S proteasome, we co-expressed Myc-StDeSI2 and GFP-Avr8 in *N. benthamiana* leaves and treated them with the proteasome inhibitor MG132 12 h prior to harvesting samples. We observed that MG132 treatment restored StDeSI2 protein abundance to levels similar to those in the control

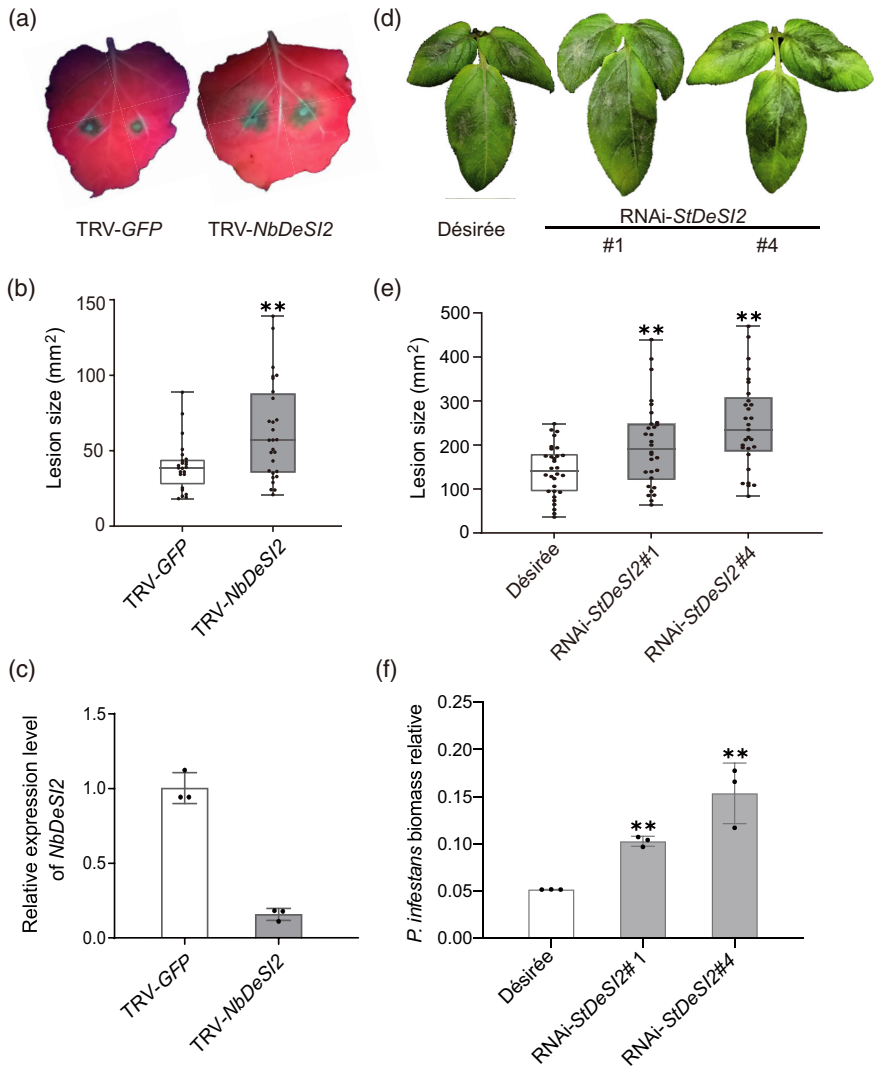

Figure 4. Silencing of *DeSI2* enhances *Phytophthora infestans* colonization in both *Nicotiana benthamiana* and potato.
(a) Representative photographs of *N. benthamiana* leaves of TRV-*NbDeSI2* and control TRV-*GFP* infected with *P. infestans* isolate 88069 at 7 days post-inoculation (dpi).
(b) The mean lesion size at 7 dpi is significantly larger in the TRV-*NbDeSI2* leaves compared with TRV2-*GFP* control. The lesion size data are shown as means with SD ($n \geq 25$).
(c) Relative expression of *NbDeSI2* is notably lower in TRV-*NbDeSI2* plants than in TRV2-*GFP* plants of *N. benthamiana*.
(d) Representative photographs of the Désirée control and two Désirée-*StDeSI2* RNAi lines #1 and #4 infected with a *P. infestans* isolate EC-1 at 5 dpi.
(e) The mean lesion size is significantly larger in leaves of Désirée-*StDeSI2* RNAi transformants than that in the Désirée control leaves at 5 dpi. The lesion size data are shown as means with SD ($n \geq 29$).
(f) The relative *P. infestans* 88069 biomass significantly increases in two Désirée-*StDeSI2* RNAi transformants #1 and #4 compared with the Désirée control. Independent experiments have been conducted at least three times with similar results. Student's *t*-test was used for the statistical analysis, and $^{**}P < 0.01$.

GFP-EV/Myc-StDeSI2, indicating that AVR8 destabilizes StDeSI2 through 26S proteasome-mediated degradation (Figure 6a,b). This finding was further confirmed by the Split-LUC experiment (Figure 6c,d).

In additional experiments, we tested different concentrations of GFP-AVR8 (OD_{600} = 0.01, 0.3, 1) with Myc-StDeSI2 (OD_{600} = 0.3) in *N. benthamiana*, with and without MG132 (100 mM). Our results demonstrated that StDeSI2 levels decreased significantly with increasing concentrations of GFP-AVR8 (OD_{600} = 0.3 to OD_{600} = 1) in the absence of MG132, and that the lowest concentration of GFP-AVR8 (OD_{600} = 0.01) did not result in detectable protein levels. Importantly, MG132 prevented the degradation of StDeSI2 (Figure S6), suggesting that AVR8 destabilizes StDeSI2 in a dose-dependent manner.

Furthermore, we found that pre-treatment with MG132 did not affect the mRNA expression level of StDeSI2 (Figure 6e). Thus, we conclude that AVR8 destabilizes the StDeSI2 protein via 26S proteasome-mediated degradation without affecting its mRNA level.

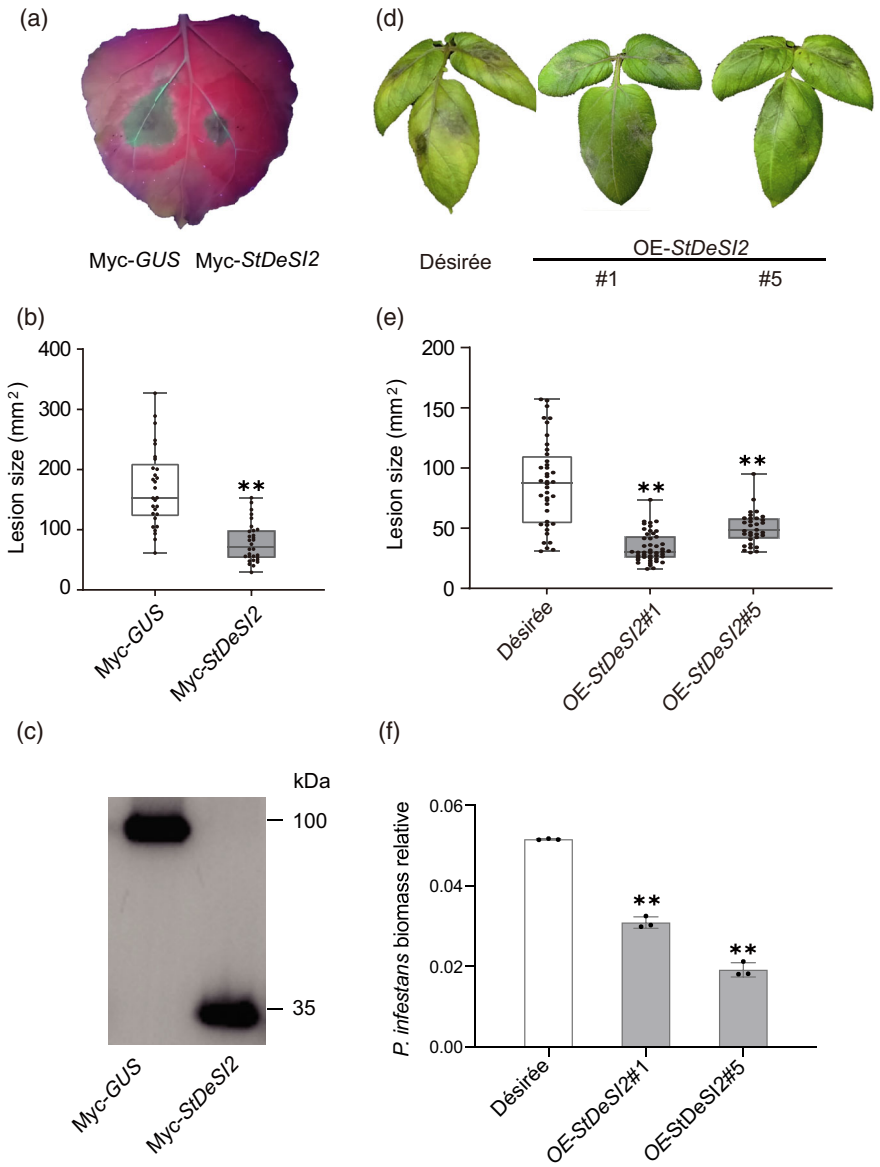

Figure 5. Overexpression of *StDeSI2* attenuates *Phytophthora infestans* colonization in both *Nicotiana benthamiana* and potato.
(a) Representative photographs of *N. benthamiana* leaves infected with a *P. infestans* isolate 88069 following overexpression of *Myc-StDeSI2* on the right side and *Myc-GUS* constructs on the left side of the midvein at 7 days post-inoculation (dpi).
(b) The mean lesion size of *Myc-StDeSI2*-overexpressing plants is reduced by nearly half the size compared with that of the *Myc-GUS* control at 7 dpi. The lesion size data are shown as means with SD ($n \geq 29$).
(c) Immunoblot shows the intactness of the Myc-StDeSI2 fusion protein. Marker size is indicated on the right in kDa.
(d) Representative photographs of the Désirée control and two Désirée-*StDeSI2* transformants #1 and #5 infected with a *P. infestans* isolate EC-1 at 5 dpi.
(e) The bar graph shows significantly reduced lesion sizes of Désirée-*StDeSI2* transformants #1 and #5 compared with the Désirée control at 5 dpi. The lesion size data are shown as means with SD ($n \geq 32$).
(f) The relative *P. infestans* 88069 biomass significantly decreases in two Désirée-*StDeSI2* transformants #1 and #5 compared with the Désirée control. Independent experiments have been conducted at least three times with similar results. Student's *t*-test was used for the statistical analysis, and $^{**}P < 0.01$.

StDeSI2 is involved in the regulation of plant defense-related genes

The above results demonstrate that StDeSI2 positively regulates plant resistance against *P. infestans*. To investigate how StDeSI2 regulates plant resistance, we performed the transcriptome profiling of Désirée and the *StDeSI2* RNAi transformant #10 on Illumina pair-end sequencing platform. Overall, 2393 genes were identified as differentially expressed genes (DEGs) in the Désirée-*StDeSI2* RNAi transformant #10 with the criteria of fold change > 4 and $P \leq 0.05$ (Table S3). This set included 1345 downregulated and 1048 upregulated genes, accounting for 56.2% and

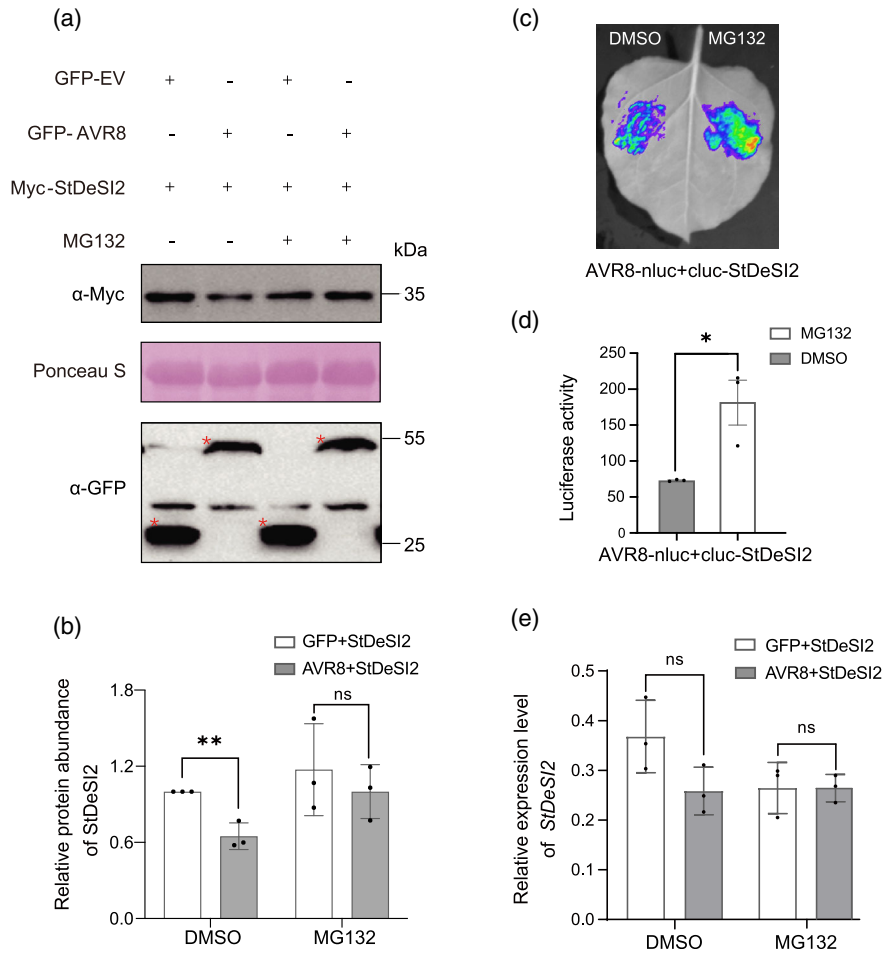

Figure 6. AVR8 destabilizes StDeSI2 protein *in planta*.
(a) Western blot detecting the protein stability of StDeSI2. The Myc-StDeSI2 construct was co-infiltrated with GFP-EV/GFP-AVR8 in *Nicotiana benthamiana*. Then leaves were infiltrated with DMSO or MG132 (100 mM) and, after 12 h, samples were collected, respectively. Co-infiltration sample pairs were harvested and detected by anti-GFP and anti-Myc antibodies. Ponceau S, Ponceau staining as the membrane loading control.
(b) The protein abundance of StDeSI2 was quantified with the results of three independent experiments by co-expressing AVR8 with and without MG132. The intensities of the Myc-StDeSI2 bands were quantitated by Photoshop CS6.
(c, d) Co-expression of the AVR8-nluc/cluc-StDeSI2 pair with MG132 significantly enhanced the luciferase catalytic activity compared with the pair without MG132. The graph shows the quantification of luciferase activity on the leaf.
(e) The relative expression level of *StDeSI2* was determined by quantitative reverse transcriptase-polymerase chain reaction (qRT-PCR). The qRT-PCR values were normalized to the transcript level of *Actin*. Independent experiments have been conducted at least three times with similar results. Student's *t*-test was used for the statistical analysis. ns, not significant.

43.8% of the total DEGs, respectively (Figure 7a). Then we took gene ontology (GO) analysis of the 2393 genes. Among the top 15 GO items, four related to defense responses, including defense response to bacterium or fungus, and cell death. In total, there are 118 unique DEGs for the four defense-related items, 45 are up- and 73 are downregulated (Figure 7b; Table S4).

Twelve defense-related genes, including *Stmpk3*, *Stsobir1*, *Stcerk1*, *Sthsp70-1*, *Stwrky53*, *Stnac71*, *Stlox1*, *Stcrk25*, *Stcar4*, *Stgso1*, *Strps5* and *Sttmm*, were chosen to further verify the RNA-seq data in another Désirée-*StDeSI2* RNAi transformant #11 by qRT-PCR (Table S5). RNA was isolated from the leaves and reverse-transcribed into cDNA. *Actin* was used as an internal control. Except for *Strps5* and *Sttmm*, the expression level of the other genes is 2–67-fold decreased in the RNAi transformant #11 compared with the control Désirée plants, which showed good consistency with RNA-seq data (Figure 7c). These results further prove that *StDeSI2* plays a vital role in plant immunity.

Silencing of *StDeSI2* attenuates early PTI responses in potato

To detect whether StDeSI2 is involved in the PTI signaling pathway, we investigated whether the silencing of *StDeSI2* affected the early expression of the PTI marker genes *Stpti5*, *Stacre31*, *Stwrky7* and *Stwrky8* (Nguyen et al., 2010; Wang et al., 2018). Entire leaves of both Désirée and

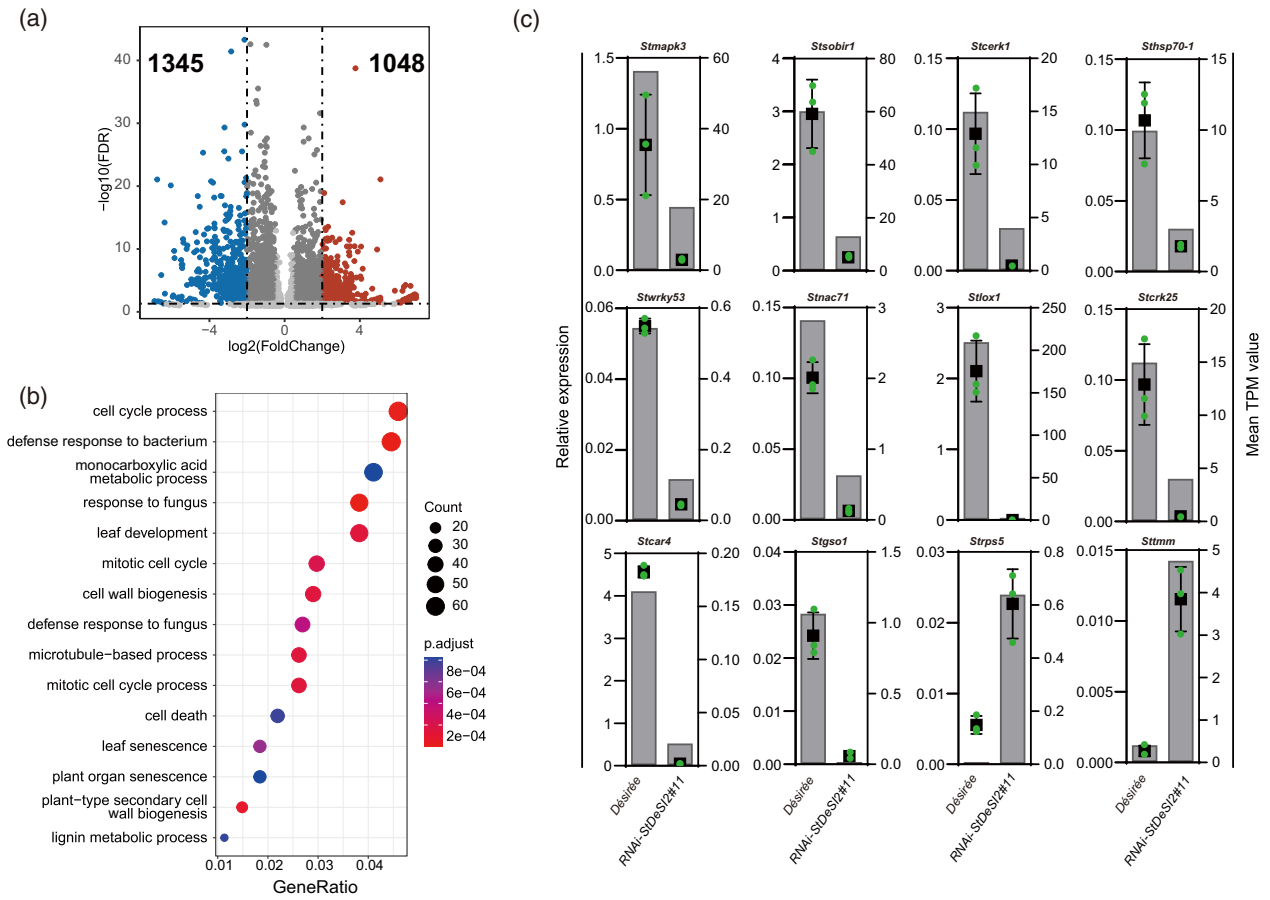

Figure 7. Silencing of *StDeSI2* largely affects the expression of defense-related genes.
(a) The volcano plot shows the differentially expressed genes (DEGs) in Désirée-*StDeSI2* RNAi transformant #10. In total, 1345 genes are downregulated and 1048 upregulated genes with the criteria of fold change > 4 and $P \leq 0.05$. Downregulated genes are presented in blue, and upregulated genes are in red.
(b) Gene ontology (GO) analysis of the DEGs from the Désirée-*StDeSI2* RNAi transformant #10 plants. The *x*-axis shows the percentages of gene counts in the specific pathway of the total DEGs, and the *y*-axis represents different pathways.
(c) Relative expression of 12 genes from the DEGs is in good consistency with that in another Désirée-*StDeSI2* RNAi transformant #11. The left *y*-axis and plots show the quantitative reverse transcriptase-polymerase chain reaction (qRT-PCR) values normalized to the transcript level of *Actin*. The right *y*-axis and gray bars show the mean TPM values. Primers used in this study are listed in Table S1.

Désirée-*StDeSI2* RNAi transformant #11 were infiltrated with *P. infestans* CF, which was used to provide PAMPs, including a variety of elicitins, etc. (McLellan et al., 2013; Saubeau et al., 2014). We found that the expression of the four PTI marker genes is upregulated from 15 min after CF induction, mostly peaked at 60 min, and then fell at 180 min (Figure 8). Compared with the expression of four marker genes in Désirée, their expression in Désirée-*StDeSI2* RNAi transformant #11 was significantly lower especially at 60 min after CF infiltration. The result indicates that StDeSI2 positively regulates PTI transcriptional response.

DISCUSSION

AVR8 is the avirulence protein that leads to hypersensitive cell death when co-expressed with R8 (Jo, 2013; Rietman et al., 2012). Effectors usually display dual roles, and here we show that AVR8 plays a role in virulence and promotes colonization of *P. infestans* in both *N. benthamiana* and potato (Figure 1). By Y2H library screening and three protein–protein interaction methods, we identified a host target of AVR8, which is a deSUMOylating isopeptidase namely, StDeSI2 (Figure 2) that co-localized with AVR8 in the cytoplasm (Figure 3). By transient and stable transformation, we proved that StDeSI2 functions as a positive regulator in plant immunity (Figures 4, 5, S4 and S5).

Previously, over a dozen *P. infestans* RXLR effectors have been studied for their virulence role, for example, to bind and alter the stability, activity or subcellular localization of a variety of host proteins, including proteases, kinases, phosphatases, transcription factors, ubiquitin ligases, RNA binding proteins, autophagy-related proteins and vesicle transport-related proteins (He et al., 2020; Petre et al., 2021). Here we provided evidence that AVR8

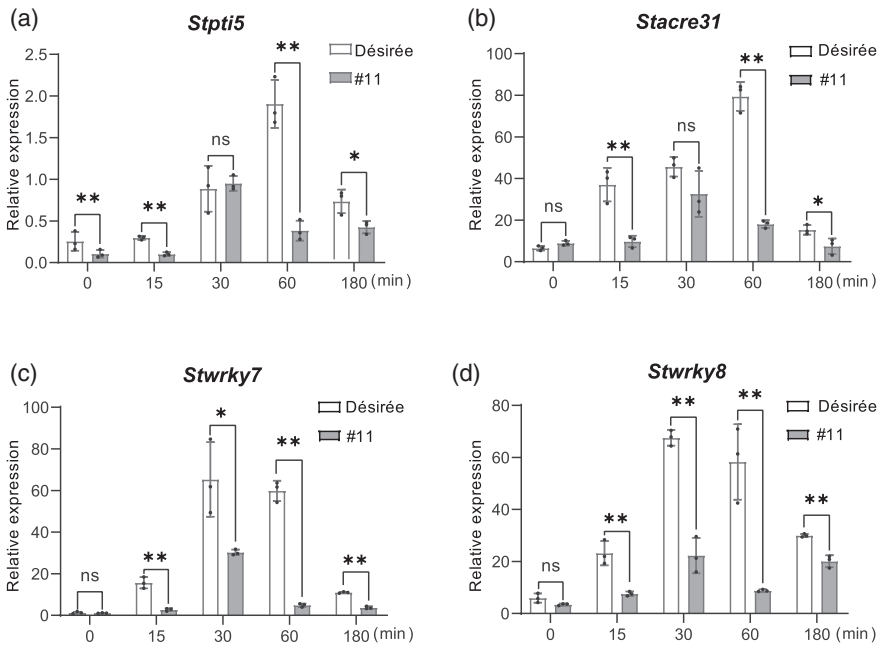

Figure 8. Silencing of *StDeSI2* attenuates early expression of four pathogen-associated molecular pattern-triggered immunity (PTI) marker genes in potato. (a–d) Expression levels of *Stpti5*, *Stwrky7*, *Stwrky8* and *Stacre31* in Désirée and the RNAi-*StDeSI2* #11, respectively, at 0 min (immediately after infiltration), 15 min, 30 min, 60 min and 180 min after *Phytophthora infestans* culture filtrate (CF) infiltration. The quantitative reverse transcriptase-polymerase chain reaction (qRT-PCR) values were normalized to the transcript level of *Actin*. Student's *t*-test was used for the statistical analysis. $^{**}P < 0.01$, $^{*}P < 0.05$ and ns, not significant.

destabilizes a desumoylation component StDeSI2, suggesting that this pathogen uses effectors to hijack desumoylation, a cellular process that is not only essential for normal plant development but also plant defense (Morrell & Sadanandom, 2019). These findings will enlarge our knowledge of how *P. infestans* manipulates plant immunity.

Actually, the importance of sumoylation in defense signaling has previously been proposed based on some evidence (Stulemeijer & Joosten, 2008). The best evidence originates from the observation that two bacterial effectors interfere with the host sumoylation cascade. The *Xanthomonas campestris* effector XopD, encoding an active cysteine protease, specifically desumoylates host proteins, thereby most likely interfering with the host defense signaling cascade upon infection (Hotson et al., 2003). Another effector from *X. campestris*, AVRXv4, requires its protease activity to reduce the amount of SUMO-conjugated proteins in the host cell, which leads to the suppression of localized cell death in inoculated plants (Roden et al., 2004). However, so far, effectors with a direct role in the sumoylation mechanism have not been identified for oomycetes (He et al., 2020, Petre et al., 2021). In this study, we show that an RXLR effector AVR8 of the oomycete pathogen *P. infestans* interferes with the host desumoylation function. The above results indicate that both sumoylation and desumoylation are important in defense signaling. DeSI3a in *Arabidopsis* has been reported as a negative regulator (Orosa et al., 2018), whereas in this study we show that StDeSI2 has a positive regulator of PTI. The opposite roles in PTI response among diverse DeSI family members point to fine-tuning and the importance of these activities through evolution. Based on our results, we hypothesized that AVR8 indirectly inhibits the expression of defense-related genes by destabilizing DeSI2, thereby reducing plant disease resistance. Our findings will be discussed below and incorporated into the model (Figure 9).

Because StDeSI2 is located in the cytoplasm, we hypothesized that it may desumo a signal component in the cytoplasm that further regulates the expression of the defense-related genes. Indeed, in this study, according to our RNA-seq analysis of Désirée-*StDeSI2* RNAi transformant #10, four GO items of the top 15 are related to defense responses, which include 118 unique DEGs with 45 upregulated and 73 downregulated (Figure 7b; Table S4). Moreover, the expression of four PTI marker genes was downregulated in the Désirée-*StDeSI2* RNAi transformant #11 (Figure 8), which indicates that the hypothesized component could be involved in the PTI pathway. However, because silencing of *DeSI2* does not affect the cell death response triggered by R8/AVR8, DeSI2 is likely not involved in the effector-triggered immunity pathway (Figure S3).

A transcriptional repressor-BZEL [BTB (Broad complex, tramtrack, bric-a-brac)-ZF (zinc-finger) protein expressed in effector lymphocytes] was described as the

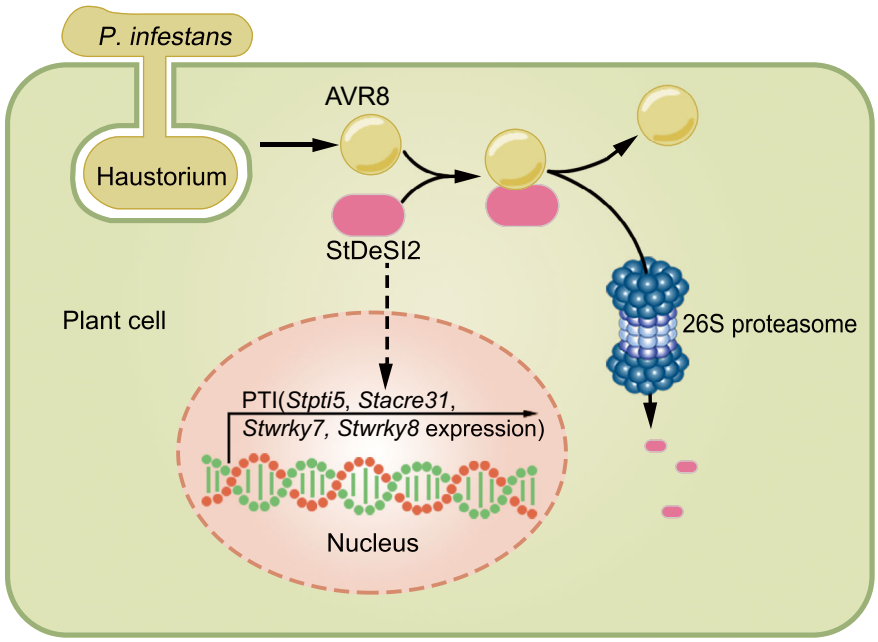

Figure 9. A *Phytophthora infestans* RXLR effector AVR8 destabilizes a potato desumoylating isopeptidase (StDeSI2) protein through the 26S proteasome and attenuates the expression of pathogen-associated molecular pattern-triggered immunity (PTI) marker genes including *Stpti5*, *Stacre31*, *Stwrky7* and *Stwrky8*.

substrate of DeSI-1 in mice and binds to the promoter of target genes to suppress their transcription (Shin et al., 2012). Thus, we hypothesize that the substrate of StDeSI2 in potato may play a similar role. In human beings, *DeSI-2* (*PNAS-4*) was identified as an apoptosis-related gene, which regulates the cell cycle (Yuan et al., 2015). Among the top 15 GO items of our RNA-seq analysis, three are related to the cell cycle (Figure 7), suggesting that the target of StDeSI2 could also potentially be involved in the cell cycle. However, because experimental evidence for the target protein of DeSI2 is lacking so far, further studies would be required. Subsequently, exploring the relation to pathogen progression may provide novel molecular targets against *Phytophthora* pathogens.

Overall, a better understanding of the contribution of *Avr8* to the viability or host colonization of *P. infestans* will help us design more targeted strategies to improve crop disease resistance. For example, the host-induced gene silence technique could be used to silence *Avr8*. Furthermore, the newly identified defense-related deSUMOylating isopeptidase StDeSI2 also provided a good target for resistance manipulation. While R protein-mediated resistance is often short-lived, subtle manipulation of effector targets may provide more durable plant resistance. In the future, we can explore the interaction sites of AVR8 and StDeSI2, and modify them with gene-editing tools to escape the recognition to restrain *P. infestans* infection while not affecting the function of StDeSI2.

EXPERIMENTAL PROCEDURES

Plant materials and transgenic plants generation

A potato cultivar Désirée was used for transformation in this study. For overexpression constructs, the *Avr8* (Pi07558) without signal peptide sequence was amplified from *P. infestans* isolate 88069 and cloned into the binary expression vector pH7LIC9.0-N-MYC as well as vectors for other aims in this study. The *StDeSI2* (Soltu.DM.03G018360.1) gene was amplified using the cDNA of a potato cultivar E-potato 3 (E3) infected with *P. infestans* and cloned into the binary expression vectors pB7WGF2 and pH7LIC9.0-N-MYC. For the RNAi construct, the interference fragment was designed in the non-conserved regions of *StDeSI2* and cloned into the vector pHellsgate 8. All the constructs were transferred into *Agrobacterium tumefaciens* strain GV3101 for potato genetic transformation. Désirée was cultured in the 3% Murashige and Skoog (MS) medium under a 16 h/8 h light and dark cycle at 22°C for 3–4 weeks, and *in vitro* stems were used as explants. They were infected with constructs containing target genes and screened on a differential medium (2 mg L^{-1} NAA, 1 mg L^{-1} 6-BA, pH 5.8). Then, buds from the callus were transferred to a root generation medium (200 mg L^{-1} Cef, 200 mg L^{-1} Tim, 75 mg L^{-1} Kan, 0.25 mg L^{-1} BSS, pH 5.8). Potential positive transgenic plants were double-checked in the root generation medium. The expression level of the transgenic plants was checked by specific primers using qRT-PCR. Primer sequences used in this study are listed in

Table S1. Two-week-old transgenic seedlings were transferred in pots in the greenhouse with a controlled environment under a 16 h/8 h light and dark cycle at 22°C.

Nicotiana benthamiana plants were grown in the growth chamber under a 16 h/8 h light and dark cycle at 24°C. Seedlings at a 2-week-old stage were used for VIGS, and leaves from 4/5-week-old plants were used for agroinfiltration assay, i.e. split luciferase assay, Co-IP and confocal microscopy.

Phytophthora infestans infection assay

Two *P. infestans* isolates 88069 and EC-1 were used for the infection assay. They were grown on Rye agar media plates at 16°C for 2 weeks for propagation. Spores were harvested by washing the plates with sterilized distilled water and adjusting the concentration to 8×10^4 sporangia ml^{-1} for potato inoculation, and 1.5×10^5 sporangia ml^{-1} for *N. benthamiana*. Five to 6-week-old potato plants were used for the infection assay. The third–fifth compound leaves counted from the uppermost were detached, and spot-inoculated with 10 μL sporangia suspension of *P. infestans* isolate onto the abaxial side of detached leaves. They were kept moist in sealed boxes. Lesions were measured when properly expanded at 5–7 dpi. For *N. benthamiana*, the 5-week-old fully developed leaves were infiltrated with *Agrobacterium* harboring pB7WGF2-*Avr8* and pH7LIC-*StDeSI2*. Then leaves were detached at 2 dpi for infection assay. The spore suspension was spot-inoculated at the abaxial side of *N. benthamiana* leaves within the agroinfiltration site. They were kept in sealed boxes to keep them moist. Lesions were measured as mentioned above.

Phylogenetic tree reconstruction

Sequences, including the unique Peptidase_C97 (PF05903) domain of the DeSI family, were downloaded from the Pfam database. The HMMER 3.0 software was used to search all genes containing this domain from the potato genome of DM v6.1 and the *N. benthamiana* genome of Niben V1.01. DeSI family members of *Arabidopsis* were obtained from the Arabidopsis Information Resource (TAIR), which were annotated as PPPDE putative thiol peptidase. Human DeSI-1 and DeSI-2 sequences were obtained from the UniProt. A maximum-likelihood tree of DeSI family members was inferred using a concatenation approach in IQ-TREE2 (v2.2.0) with an edge-linked proportional partition model bootstrapped 1000 times with ultrafast bootstraps (Minh et al., 2020). Each partition's substitution model was determined using the MFP option (Kalyaanamoorthy et al., 2017). The resulting tree was visualized using MEGA11 and annotated in Adobe Illustrator 2022. The tree was rooted in Human DeSI-2.

Yeast-two-hybrid assay

A potato cDNA library infected by *P. infestans* described previously (McLellan et al., 2013) was used to screen the potential target of AVR8. *Avr8* without a signal peptide and the ED of *Avr8* were amplified with primers attB1-*Avr8*/attB2-*Avr8*, attB1-ED/attB2-*Avr8*, respectively (Table S1). Then they were cloned to the 'bait' vector pDEST32 and transformed into yeast strain Mav203. pDEST32-ED bearing yeast was used to prepare competent cells, which were transformed with the cDNA library plasmid using the Invitrogen ProQuest system. All transformants were spread on the SD/-Trp-Leu-His selection medium plates with 25 mM 3-AT (3-amino-1,2,4-triazole). Candidate clones were sequenced and then analyzed using the NCBI database. To further confirm the interaction between AVR8 and StDeSI2, the coding sequence of *StDeSI2* was cloned into the 'prey' vector pDEST22, and AVR2 was used as a negative control. For each pair to be verified, 'bait' and 'prey' vectors were co-transformed into Mav203 competent cells. Interactions were confirmed by testing the transformants on the SD/-Trp-Leu-His medium and the X-β-gal assay.

Co-immunoprecipitation

N-terminal *GFP*-tagged *Avr8* and N-terminal *HA*-tagged *StDeSI2* constructs were co-infiltrated at a 1:1 ratio of OD_{600} = 0.3 in leaves of 5-week-old *N. benthamiana*. Leaves were harvested using a 1-cm-diameter puncher 48 h post-infiltration, and quick-frozen in liquid nitrogen. Total proteins were extracted with the extraction buffer [GTEN (10% glycerol, 25 mM Tris, pH 7.5, 1 mM EDTA, 150 mM NaCl), protease inhibitor cocktail Complete Mini tablets (Roche), 0.2% Nonidet P40, 10 mM dithiothreitol (DTT) and 1 mM PMSF]. For input, 50 μL supernatant was added to 50 μL 2 × sodium dodecyl sulfate–polyacrylamide gel electrophoresis (SDS–PAGE) loading buffer with 20 mM DTT and boiled at 95°C for 10 min. For Co-IP, 25 μL GFP magnetic beads were washed three times with wash buffer (GTEN and 3 mM PMSF). Crude proteins were incubated with GFP beads at 4°C for 2 h in a low-speed rotator. The precipitated protein on the beads was gathered by the magnetic rank and washed three times with wash buffer; 50 μL 2 × SDS–PAGE loading buffer was used to resuspend the precipitated protein. Proteins were detected by immunoblot using the anti-GFP and anti-HA antibodies (Bioyears, Beijing).

Split luciferase (Split-LUC) in *Nicotiana benthamiana*

For split luciferase assay, the full length of *Avr8* was amplified with primers JW771-Avr8-F/R and cloned to the vector JW771 with N-terminal luciferase, while *StDeSI2* to the vector JW772 with C-terminal luciferase. Recombinant constructs were transformed to *Agrobacterium* GV3101 and co-infiltrated in 4-week-old *N. benthamiana* leaves with OD_{600} = 0.3 at a ratio of 1:1. JW771-NPR3 and JW772-NPR4 were used as a positive control (Fu et al., 2012), while JW771-EV and JW772-EV as a negative control. D-Luciferin potassium solution (Sigma-Aldrich; 1 mM), the substrate of

luciferase, was put on the abaxial side of detached *N. benthamiana* leaves 48 h post-agro-infiltration in the dark for about 10 min. A CCD imaging apparatus was used to capture luminescence images.

Confocal microscopy

For confocal microscopy, a recombinant vector of StDeSI2 fused with an N-terminal RFP tag was constructed and transformed into the *Agrobacterium* GV3101. *GFP-Avr8* and *RFP-StDeSI2* constructs were infiltrated in *N. benthamiana* leaves at OD_{600} = 0.1 in a 1:1 ratio together and separately. Subcellular localization was conducted 48 h post-infiltration with a confocal microscope SP8 (Leica). The fluorescence intensity was quantified using the 'Plot Profile' tool in ImageJ 1.53e for different fluorescence channels, and the results were visualized using GraphPad Prism 7. Protein stability was detected as mentioned above.

Virus-induced gene silencing

A 304-bp fragment near the N-terminal of *NbDeSI2* was selected to make a VIGS construct TRV2-*NbDeSI2* to avoid off-target. TRV-GFP was used as a negative control. The suspension of TRV2-recombinant vectors and TRV1 was mixed in a ratio of 1:1 at a final OD_{600} = 0.6, kept in the dark for 1–6 h, and infiltrated into the leaves of 2-week-old *N. benthamiana*. The silencing efficiency of *NbDeSI2* was detected using qRT-PCR. Three weeks later, the third–fifth leaves counted from the top were detached for *P. infestans* infection assay. Primers used in this study are listed in Table S1.

RNA-seq and qRT-PCR

Désirée and Désirée-*StDeSI2* RNAi transformant plants were grown in the greenhouse under controlled conditions. Three–five compound leaves were collected from 5-week-old plants and subjected to RNA extraction using a Plant Total RNA Kit (ZOMANBIO, Beijing). Three replicates per sample were sent to the company Novogen (Beijing) for RNA sequencing using the Illumina platform. DM_1–3_516_R44_potato. v6.1 in the International Potato Genome Sequencing Consortium (PGSC) website was used as the reference genome. Clean reads generated were used for assembly and aligned with the potato genome sequence by Hisat2 (Ver 2.2.1). Differential expression genes were analyzed by Stringtie (Ver2.2.0), and mapping reads were exported by R package DESeq2. Principal component analysis (PCA) was performed by factoMineR. GO analysis was performed by transforming DEGs into TAIR ID. Genes were enriched by Org.At.tair.db and demonstrated by clusterProfiler.

Désirée-*StDeSI2* RNAi transformant #11 was used for qRT-PCR analysis. According to the manufacturer's instructions, cDNA synthesis was conducted using the reverse transcriptase kit (Abm). qRT-PCR was performed on PCR machine ABI7300 (Applied Biosystems) using the Blastaq 2 × qPCR Mastermix (Abm), and *Actin* was used as an internal control. The threshold cycle (CT) value was quantified using the $2^{-\Delta CT}$ method. Primers of defense-related genes tested in the qRT-PCR assay are listed in Table S1.

Phytophthora infestans biomass detection

Phytophthora infestans hypha biomass was measured by qPCR. Total DNA was extracted from leaves around inoculated sites at 5 dpi. The relative hypha biomass was quantified by normalizing the *P. infestans ef2α* gene values with the potato *StEF1α* gene values.

Phytophthora infestans CF preparation

For preparing CF, *P. infestans* mycelia and sporangia were cultured in Plich liquid medium (0.5 g KH_2PO_4, 0.25 g $MgSO_4{\cdot}7H_2O$, 1 g Asparagine, 1 mg Thiamine, 0.5 g Yeast extract, 10 mg β-sitosterol and 25 g Glucose) for 4 weeks at 16°C in the dark.

AUTHOR CONTRIBUTIONS

RJ, QH, JS, ZL, JY, KH, HL, YM, JW and JD performed experiments and analyzed data; RJ, QH, JS, ZL, JY, KH, HL, YM, JW, ZT, BS, CX and JD designed experiments; RJ, QH, ZT, BS, CX and JD supervised; RJ, QH, JS, VGAAV, CX and JD wrote the manuscript.

ACKNOWLEDGEMENTS

The authors thank Paul R.J. Birch for providing the yeast library, Feng Li for providing the pH7LIC vector, and Zhibing Lai for valuable suggestions and for improving the manuscript. The work was partially supported by the National Science Foundation of China (31401436), and the Key-Area Research and Development Program of Guangdong Province (2020B020219002).

CONFLICT OF INTEREST

The authors declare no competing financial interests.

SUPPORTING INFORMATION

Additional Supporting Information may be found in the online version of this article.

Figure S1. Phylogenic analysis and protein structure of DeSI family members. (a) A maximum-likelihood tree of DeSI family members from potato (*Solanum tuberosum*), *Nicotiana benthamiana*, and proteins with high homology in *Arabidopsis thaliana* and *Homo sapiens*. Bootstrap values exceeding 50% are indicated at the nodes, and branch lengths represent weighted amino acid substitutions. (b) Protein structures of DeSI family members. Blocks in red, yellow and green represent three different conserved domains in DeSI family members. (c) Amino acids of three conserved domains in DeSI family members.

Figure S2. Effects of silencing *NbDeSI2* in *N. benthamiana* plants. (a) Alignment of *StDeSI2*, *NbDeSI2A* and *NbDeSI2B* cDNA sequence. VIGS fragments of *N. benthamiana* are depicted in a red line. (b) No obvious phenotypic variation between TRV2-*NbDeSI2* and the TRV2-*GFP* control was found. Photographs were taken at 3 weeks post agro-coinfiltration of TRV1 with three

constructs TRV2-*PDS*, TRV2-*GFP* and TRV2-*NbDeSI2*, respectively. TRV2-*PDS* was used as an environmental control. (c) Relative expression levels of *NbDeSI2* were detected by qRT-PCR in TRV2-*NbDeSI2* and the TRV2-*GFP* control plants of *N. benthamiana*. Samples were collected at 3 weeks post agro-infiltration. White and gray columns show the *NbDeSI2* expression level in TRV2-*GFP* control and TRV2-*NbDeSI2*-treated plants, respectively. Numbers 1–3 represent three biological replicates. Student's *t*-test was used for the statistical analysis, and $^{**}P < 0.01$.

Figure S3. Silencing *NbDeSI2* does not affect R8/AVR8 triggered cell death *in N. benthamiana*. (a) Diagram of a leaf showing infiltration sites in (b) and (c). *Agrobacterium* carrying pB7WGF2-R8/pB7WGF2-AVR8, pB7WGF2-Cf-4/pB7WGF2-AVR4 (Joosten et al., 1994) and pGR106-INF1, respectively, as well as *P. infestans* culture filtrate (CF) triggered cell death responses on TRV-*NbDeSI2*-treated *N. benthamiana* leaves (b) as well as on TRV-*GFP* control plants (c), while their empty vectors pGR106-EV (negative control on the left panel) and pB7WGF2-EV (negative control on the right panel) did not trigger any obvious symptoms.

Figure S4. Silencing of *StDeSI2* enhances *P. infestans* colonization in potato. (a) Representative photographs of Désirée-*StDeSI2* RNAi transformants after 7 weeks of growth in the pot. (b) The mean lesion size is significantly larger in leaves of four Désirée-*StDeSI2* RNAi transformants #1, #4, #5 and #6 than that in the Désirée control leaves infected with a *P. infestans* isolate EC-1 at 5 dpi. The lesion size data are shown as means with SD ($n \geq 29$). (c) The mean lesion size is significantly larger in leaves of four Désirée-*StDeSI2* RNAi transformants #7, #8, #10 and #11 than that in the Désirée control leaves infected with a *P. infestans* isolate 88069 at 5 dpi. The lesion size data are shown as means with SD ($n \geq 29$). (d) Relative expression of *StDeSI2* in eight Désirée-*StDeSI2* RNAi transformants. Student's *t*-test was used for the statistical analysis, and $^{*}P < 0.05$. (e) Relative expression of *StDeSI2* in Désirée-*StDeSI2* RNAi transformants #4 and Désirée control infected with *P. infestans* inoculation at 3–5 dpi.

Figure S5. Overexpression of *StDeSI2* attenuates *P. infestans* colonization in potato. (a) Representative photographs of Désirée-*StDeSI2* transformants after 7 weeks growing in the pot. (b) The mean lesion size is significantly smaller in leaves of three Désirée-*StDeSI2* transformants #1, #4 and #5 than that in the Désirée control leaves infected with a *P. infestans* isolate 88069 at 5 dpi. The lesion size data are shown as means with SD ($n \geq 18$). (c) The mean lesion size is significantly smaller in leaves of four Désirée-*StDeSI2* transformants #1, #3, #4 and #5 than that in the Désirée control leaves infected with a *P. infestans* isolate EC-1 at 5 dpi. The lesion size data are shown as means with SD ($n \geq 32$). (d) Relative expression of *StDeSI2* in four Désirée-*StDeSI2* transformants. Student's *t*-test was used for the statistical analysis, and $^{**}P < 0.01$.

Figure S6. AVR8 destabilizes StDeSI2 in a dosage-dependent manner. The protein abundance of StDeSI2 was detected by Western blot. Different concentrations of GFP-AVR8 construct (OD_{600} = 0.01, 0.3, 1) were co-infiltrated with Myc-StDeSI2 (OD_{600} = 0.3) in *N. benthamiana* with and without MG132 (100 mM). The asterisk in red demonstrates the band of GFP-AVR8.

Table S1. Primers used in this study

Table S2. Similarities of all DeSI family members from human, *Arabidopsis*, potato and *Nicotiana benthamiana*

Table S3. Information of 2393 differentially expressed genes in the Désirée-*StDeSI2* RNAi transformant #10

Table S4. GO enrichment analysis of 2393 differentially expressed genes in the Désirée-*StDeSI2* RNAi transformant #10

Table S5. Information of 12 differentially expressed genes tested in Désirée-*StDeSI2* RNAi transformant #11

REFERENCES

Boevink, P.C., Wang, X., McLellan, H., He, Q., Naqvi, S., Armstrong, M.R. *et al.* (2016) A *Phytophthora infestans* RXLR effector targets plant PP1c isoforms that promote late blight disease. *Nature Communications*, **7**, 10311.

Bos, J.I.B., Armstrong, M.R., Gilroy, E.M., Boevink, P.C., Hein, I., Taylor, R.M. *et al.* (2010) *Phytophthora infestans* effector AVR3a is essential for virulence and manipulates plant immunity by stabilizing host E3 ligase CMPG1. *Proceedings of the National Academy of Sciences of the United States of America*, **107**, 9909–9914.

Bos, J.I.B., Kanneganti, T.D., Young, C., Cakir, C., Huitema, E., Win, J. *et al.* (2006) The C-terminal half of *Phytophthora infestans* RXLR effector AVR3a is sufficient to trigger R3a-mediated hypersensitivity and suppress INF1-induced cell death in *Nicotiana benthamiana*. *The Plant Journal*, **48**, 165–176.

Bozkurt, T.O., Schornack, S., Win, J., Shindo, T., Ilyas, M., Oliva, R. *et al.* (2011) *Phytophthora infestans* effector AVRblb2 prevents secretion of a plant immune protease at the haustorial interface. *Proceedings of the National Academy of Sciences of the United States of America*, **108**, 20832–20837.

Dagdas, Y.F., Belhaj, K., Maqbool, A., Chaparro-Garcia, A., Pandey, P., Petre, B. *et al.* (2016) An effector of the Irish potato famine pathogen antagonizes a host autophagy cargo receptor. *eLife*, **5**, e10856.

Dagdas, Y.F., Pandey, P., Tumtas, Y., Sanguankiattichai, N., Belhaj, K., Duggan, C. *et al.* (2018) Host autophagy machinery is diverted to the pathogen interface to mediate focal defense responses against the Irish potato famine pathogen. *eLife*, **7**, e37476.

Dong, S., Stam, R., Cano, L.M., Song, J., Sklenar, J., Yoshida, K. *et al.* (2014) Effector specialization in a lineage of the Irish potato famine pathogen. *Science*, **343**, 552–555.

Du, J. & Vleeshouwers, V.G.A.A. (2017) New strategies towards durable late blight resistance in potato. In: Chakrabarti, S. K., & Xie, C. (Eds.) *The potato genome*. Cham: Springer, pp. 161–169.

Du, Y., Chen, X., Guo, Y., Zhang, X., Zhang, H., Li, F. *et al.* (2020) *Phytophthora infestans* RXLR effector PITG20303 targets a potato MKK1 protein to suppress plant immunity. *The New Phytologist*, **229**, 501–515.

Du, Y., Mpina, M.H., Birch, P.R., Bouwmeester, K. & Govers, F. (2015) *Phytophthora infestans* RXLR effector AVR1 interacts with exocyst component sec5 to manipulate plant immunity. *Plant Physiology*, **169**, 1975–1990.

Fry, W. (2008) *Phytophthora infestans*: the plant (and *R* gene) destroyer. *Molecular Plant Pathology*, **9**, 385–402.

Fu, Z.Q., Yan, S.P., Saleh, A., Wang, W., Ruble, J., Oka, N. *et al.* (2012) NPR3 and NPR4 are receptors for the immune signal salicylic acid in plants. *Nature*, **486**, 228–232.

Gawehns, F., Cornelissen, B.J. & Takken, F.L. (2013) The potential of effector-target genes in breeding for plant innate immunity. *Microbial Biotechnology*, **6**, 223–229.

Gilroy, E.M., Taylor, R.M., Hein, I., Boevink, P., Sadanandom, A. & Birch, P.R.J. (2011) CMPG1-dependent cell death follows perception of diverse pathogen elicitors at the host plasma membrane and is suppressed by *Phytophthora infestans* RXLR effector AVR3a. *The New Phytologist*, **190**, 653–666.

Haas, B.J., Kamoun, S., Zody, M.C., Jiang, R.H., Handsaker, R.E., Cano, L.M. *et al.* (2009) Genome sequence and analysis of the Irish potato famine pathogen *Phytophthora infestans*. *Nature*, **461**, 393–398.

He, J., Ye, W., Choi, D.S., Wu, B., Zhai, Y., Guo, B. *et al.* (2019) Structural analysis of *phytophthora* suppressor of RNA silencing 2 (PSR2) reveals a conserved modular fold contributing to virulence. *Proceedings of the National Academy of Sciences of the United States of America*, **116**, 8054–8059.

He, Q., McLellan, H., Boevink, P.C. & Birch, P.R.J. (2020) All roads lead to susceptibility: the many modes of action of fungal and oomycete intracellular effectors. *Plant Communications*, **1**, 100050.

He, Q., McLellan, H., Hughes, R.K., Boevink, P.C., Armstrong, M., Lu, Y. *et al.* (2019) *Phytophthora infestans* effector SFI3 targets potato UBK to suppress early immune transcriptional responses. *The New Phytologist*, **222**, 438–454.

He, Q., Naqvi, S., McLellan, H., Boevink, P.C., Champouret, N., Hein, I. *et al.* (2018) Plant pathogen effector utilizes host susceptibility factor NRL1 to

degrade the immune regulator SWAP70. *Proceedings of the National Academy of Sciences of the United States of America*, **115**, E7834–E7843.
Hickey, C.M., **Wilson, N.R.** & **Hochstrasser, M.** (2012) Function and regulation of SUMO proteases. *Nature Reviews Molecular Cell Biology*, **13**, 755–766.
Hotson, A., **Chosed, R.**, **Shu, H.**, **Orth, K.** & **Mudgett, M.B.** (2003) *Xanthomonas* type III effector XopD targets SUMO-conjugated proteins *in planta*. *Molecular Microbiology*, **50**, 377–389.
Jiang, R., **Li, J.C.**, **Tian, Z.D.**, **Du, J.**, **Armstrong, M.**, **Baker, K.** ***et al.*** (2018) Potato late blight field resistance from QTL *dPI09c* is conferred by the NB-LRR gene *R8*. *Journal of Experimental Botany*, **69**, 1545–1555.
Jo, K.R. (2013) Unveiling and deploying durability of late blight resistance in potato: Wageningen University.
Joosten, M.H., **Cozijnsen, T.J.** & **De Wit, P.J.** (1994) Host resistance to a fungal tomato pathogen lost by a single base-pair change in an avirulence gene. *Nature*, **367**, 384–386.
Kalyaanamoorthy, S., **Minh, B.Q.**, **Wong, T.K.F.**, **von Haeseler, A.** & **Jermiin, L.S.** (2017) ModelFinder: fast model selection for accurate phylogenetic estimates. *Nature Methods*, **14**, 587–589.
King, S.R.F., **McLellan, H.**, **Boevink, P.C.**, **Armstrong, M.R.**, **Bukharova, T.**, **Sukarta, O.** ***et al.*** (2014) *Phytophthora infestans* RXLR effector PexRD2 interacts with host MAPKKK epsilon to suppress plant immune signaling. *Plant Cell*, **26**, 1345–1359.
Liu, L., **Sonbol, F.M.**, **Huot, B.**, **Gu, Y.**, **Withers, J.**, **Mwimba, M.** ***et al.*** (2016) Salicylic acid receptors activate jasmonic acid signalling through a non-canonical pathway to promote effector-triggered immunity. *Nature Communications*, **7**, 13099.
McDonald, B.A. & **Linde, C.** (2002) Pathogen population genetics, evolutionary potential, and durable resistance. *Annual Review of Phytopathology*, **40**, 349–379.
McLellan, H., **Boevink, P.C.**, **Armstrong, M.R.**, **Pritchard, L.**, **Gomez, S.**, **Morales, J.** ***et al.*** (2013) An RxLR effector from *Phytophthora infestans* prevents re-localisation of two plant NAC transcription factors from the endoplasmic reticulum to the nucleus. *PLoS Pathogens*, **9**, e1003670.
Minh, B.Q., **Schmidt, H.A.**, **Chernomor, O.**, **Schrempf, D.**, **Woodhams, M.D.**, **von Haeseler, A.** ***et al.*** (2020) IQ-TREE 2: new models and efficient methods for phylogenetic inference in the genomic era. *Molecular Biology and Evolution*, **37**, 1530–1534.
Morrell, R. & **Sadanandom, A.** (2019) Dealing with stress: a review of plant sumo proteases. *Frontiers in Plant Science*, **10**, 1122.
Murphy, F., **He, Q.**, **Armstrong, M.**, **Giuliani, L.M.**, **Boevink, P.C.**, **Zhang, W.** ***et al.*** (2018) The potato MAP3K StVIK is required for *Phytophthora infestans* RXLR effector Pi17316 to promote disease. *Plant Physiology*, **177**, 398–410.
Nayak, A. & **Muller, S.** (2014) SUMO-specific proteases/isopeptidases: SENPs and beyond. *Genome Biology*, **15**, 422.
Nguyen, H.P., **Chakravarthy, S.**, **Velasquez, A.C.**, **McLane, H.L.**, **Zeng, L.R.**, **Nakayashiki, H.** ***et al.*** (2010) Methods to study PAMP-triggered immunity using tomato and *Nicotiana benthamiana*. *Molecular Plant-Microbe Interactions*, **23**, 991–999.
Orosa, B., **Yates, G.**, **Verma, V.**, **Srivastava, A.K.**, **Srivastava, M.**, **Campanaro, A.** ***et al.*** (2018) SUMO conjugation to the pattern recognition receptor FLS2 triggers intracellular signalling in plant innate immunity. *Nature Communications*, **9**, 1–12.
Pandey, P., **Leary, A.Y.**, **Tumtas, Y.**, **Savage, Z.**, **Dagvadorj, B.**, **Duggan, C.** ***et al.*** (2021) An oomycete effector subverts host vesicle trafficking to channel starvation-induced autophagy to the pathogen interface. *eLife*, **10**, e65285.
Park, H.J., **Kim, W.Y.**, **Park, H.C.**, **Lee, S.Y.**, **Bohnert, H.J.** & **Yun, D.J.** (2011) SUMO and SUMOylation in plants. *Molecules and Cells*, **32**, 305–316.
Petre, B., **Contreras, M.P.**, **Bozkurt, T.O.**, **Schattat, M.H.**, **Sklenar, J.**, **Schornack, S.** ***et al.*** (2021) Host-interactor screens of *Phytophthora infestans* RXLR proteins reveal vesicle trafficking as a major effector-targeted process. *Plant Cell*, **33**, 1447–1471.
Raffaele, S., **Farrer, R.A.**, **Cano, L.M.**, **Studholme, D.J.**, **MacLean, D.**, **Thines, M.** ***et al.*** (2010) Genome evolution following host jumps in the Irish potato famine pathogen lineage. *Science*, **330**, 1540–1543.
Ren, Y., **Armstrong, M.**, **Qi, Y.**, **McLellan, H.**, **Zhong, C.**, **Du, B.** ***et al.*** (2019) *Phytophthora infestans* RXLR effectors target parallel steps in an immune signal transduction pathway. *Plant Physiology*, **180**, 2227–2239.
Rietman, H., **Bijsterbosch, G.**, **Cano, L.M.**, **Lee, H.R.**, **Vossen, J.H.**, **Jacobsen, E.** ***et al.*** (2012) Qualitative and quantitative late blight resistance in the potato cultivar Sarpo Mira is determined by the perception of five distinct RXLR effectors. *Molecular Plant-Microbe Interactions*, **25**, 910–919.
Roden, J., **Eardley, L.**, **Hotson, A.**, **Cao, Y.** & **Mudgett, M.B.** (2004) Characterization of the *Xanthomonas* AvrXv4 effector, a SUMO protease translocated into plant cells. *Molecular Plant-Microbe Interactions*, **17**, 633–643.
Saubeau, G., **Gaillard, F.**, **Legentil, L.**, **Nugier-Chauvin, C.**, **Ferrieres, V.**, **Andrivon, D.** ***et al.*** (2014) Identification of three elicitins and a galactan-based complex polysaccharide from a concentrated culture filtrate of *Phytophthora infestans* efficient against *Pectobacterium atrosepticum*. *Molecules*, **19**, 15374–15390.
Shin, E.J., **Shin, H.M.**, **Nam, E.**, **Kim, W.S.**, **Kim, J.H.**, **Oh, B.H.** ***et al.*** (2012) DeSUMOylating isopeptidase: a second class of SUMO protease. *EMBO Reports*, **13**, 339–346.
Stulemeijer, I.J.E. & **Joosten, M.H.A.J.** (2008) Post-translational modification of host proteins in pathogen-triggered defense signalling in plants. *Molecular Plant Pathology*, **9**, 545–560.
Turnbull, D., **Wang, H.**, **Breen, S.**, **Malec, M.**, **Naqvi, S.**, **Yang, L.** ***et al.*** (2019) AVR2 targets BSL family members, which act as susceptibility factors to suppress host immunity. *Plant Physiology*, **180**, 571–581.
Turnbull, D., **Yang, L.N.**, **Naqvi, S.**, **Breen, S.**, **Welsh, L.**, **Stephens, J.** ***et al.*** (2017) RXLR effector AVR2 upregulates a brassinosteroid- responsive bHLH transcription factor to suppress immunity. *Plant Physiology*, **174**, 356–369.
van Schie, C.C.N. & **Takken, F.L.W.** (2014) Susceptibility genes 101: how to be a good host. *Annual Review of Phytopathology*, **52**, 551–581.
Vleeshouwers, V.G.A.A., **Raffaele, S.**, **Vossen, J.H.**, **Champouret, N.**, **Oliva, R.**, **Segretin, M.E.** ***et al.*** (2011) Understanding and exploiting late blight resistance in the age of effectors. *Annual Review of Phytopathology*, **49**, 507–531.
Vossen, J.H., **van Arkel, G.**, **Bergervoet, M.**, **Jo, K.R.**, **Jacobsen, E.** & **Visser, R.G.F.** (2016) The *Solanum demissum R8* late blight resistance gene is an *Sw-5* homologue that has been deployed worldwide in late blight resistant varieties. *Theoretical and Applied Genetics*, **129**, 1785–1796.
Wang, H., **He, H.**, **Qi, Y.**, **McLellan, H.**, **Tian, Z.**, **Birch, P.R.J.** ***et al.*** (2018) The oomycete microbe-associated molecular pattern Pep-13 triggers SERK3/BAK1-independent plant immunity. *Plant Cell Reports*, **37**, 173–182.
Wang, S., **McLellan, H.**, **Bukharova, T.**, **He, Q.**, **Murphy, F.**, **Shi, J.** ***et al.*** (2019) *Phytophthora infestans* RXLR effectors act in concert at diverse subcellular locations to enhance host colonization. *Journal of Experimental Botany*, **70**, 343–356.
Wang, X., **Boevink, P.**, **McLellan, H.**, **Armstrong, M.**, **Bukharova, T.**, **Qin, Z.** ***et al.*** (2015) A host KH RNA-binding protein is a susceptibility factor targeted by an RXLR effector to promote late blight disease. *Molecular Plant*, **8**, 1385–1395.
Whisson, S.C., **Boevink, P.C.**, **Moleleki, L.**, **Avrova, A.O.**, **Morales, J.G.**, **Gilroy, E.M.** ***et al.*** (2007) A translocation signal for delivery of oomycete effector proteins into host plant cells. *Nature*, **450**, 115–118.
Win, J., **Chaparro-Garcia, A.**, **Belhaj, K.**, **Saunders, D.G.**, **Yoshida, K.**, **Dong, S.** ***et al.*** (2012) Effector biology of plant-associated organisms: concepts and perspectives. *Cold Spring Harbor Symposia on Quantitative Biology*, **77**, 235–247.
Witek, K., **Lin, X.**, **Karki, H.S.**, **Jupe, F.**, **Witek, A.I.**, **Steuernagel, B.** ***et al.*** (2021) A complex resistance locus in *Solanum americanum* recognizes a conserved *phytophthora* effector. *Nature Plants*, **7**, 198–208.
Yates, G., **Srivastava, A.K.** & **Sadanandom, A.** (2016) SUMO proteases: uncovering the roles of deSUMOylation in plants. *Journal of Experimental Botany*, **67**, 2541–2548.
Yuan, Z., **Guo, W.**, **Yang, J.**, **Li, L.**, **Wang, M.**, **Lei, Y.** ***et al.*** (2015) *PNAS-4*, an early DNA damage response gene, induces s phase arrest and apoptosis by activating checkpoint kinases in lung cancer cells. *Journal of Biological Chemistry*, **290**, 14927–14944.
Zheng, X., **Wagener, N.**, **McLellan, H.**, **Boevink, P.C.**, **Hua, C.**, **Birch, P.R.J.** ***et al.*** (2018) *Phytophthora infestans* RXLR effector SFI5 requires association with calmodulin for PTI/MTI suppressing activity. *The New Phytologist*, **219**, 1433–1446.